

Experimental and theoretical studies of the CCl + O₂ reaction

Tiancheng Xiang, Kunhui Liu, Congyun Shi, Hongmei Su *, Fanao Kong

State Key Laboratory of Molecular Reaction Dynamics, Beijing National Laboratory for Molecular Sciences (BNLMS), Institute of Chemistry, Chinese Academy of Sciences, Beijing 100080, China

Received 22 November 2006; in final form 30 January 2007

Available online 4 February 2007

Abstract

Elementary reaction of CCl radical with oxygen molecule has been investigated by time-resolved Fourier transform infrared emission spectroscopy. Product of CO was observed. The rate constant of this reaction is measured to be $2.6(\pm 0.4) \times 10^{-12} \text{ cm}^3 \text{ molecule}^{-1} \text{ s}^{-1}$. It is found that the nascent product of CO is highly vibrationally excited with an average vibrational energy of 17–18 kcal mol⁻¹. DFT calculations at the B3LYP/6-311G(d) level reveal the reaction mechanism to be mainly a barrierless addition of O₂ to CCl leading to a peroxide intermediate IM1 (CICOO). The chain-like IM1 breaks its O–O bond and Cl–C bond sequentially, forming the product of CO.

© 2007 Elsevier B.V. All rights reserved.

1. Introduction

Chlorine containing radicals play a significant role in atmospheric chemistry, such as stratospheric ozone depletion, incineration and high-temperature pyrolysis of chlorocarbon polymers [1,2]. Chlorinated methylidyne radical (CCl), a very reactive species, has been subjected to wide investigations [3–9]. Rate constants of the reactions between CCl with O₂, NO, F₂, CO, H₂O, CH₄, CCl₄, C₃H₈, H₂ and SF₆ were measured by different methods [3,4]. The rate constant for the reaction of CCl with O₂ is measured by monitoring the reactant concentration [CCl] with LIF spectroscopy to be $2.91(\pm 0.144) \times 10^{-12} \text{ cm}^3 \text{ molecule}^{-1} \text{ s}^{-1}$ [3]. Using flash-photolysis and kinetics spectroscopy method, Tyerman measured the rate constant for the same reaction to be $4.15(\pm 0.498) \times 10^{-12} \text{ cm}^3 \text{ molecule}^{-1} \text{ s}^{-1}$ [4].

Unfortunately it is lack of the knowledge of products, pathway and mechanism of this reaction in the literatures so far. In the present Letter, time-resolved Fourier transform infrared (TR-FTIR) emission spectroscopy has been

used to determine the reaction products and reaction channels. The reaction rate constant is measured again by detecting the formation of the products. The reaction mechanism is studied also theoretically by density function theory (DFT) calculation at the B3LYP/6-311G(d) level.

2. Experimental and theoretical methods

The reaction products are monitored by step-scan, time-resolved Fourier transform emission spectroscopy [10]. This is an effective technique to acquire broad-band, time-resolved spectra of multiple reactants and products simultaneously.

Step-scan FTIR spectrometer is commercially available but requires significant modification for coupling with pulsed laser and study of photolysis initiated free radical reactions. This newly upgraded machine comprises a Nicolet Nexus 870 step-scan FTIR spectrometer, Lambda Physik (LPX305i) Excimer laser and a pulse generator (Stanford Research DG535) to initiate the laser pulse and achieve synchronization of the laser with data collection, two digitizers (internal 100 KHz 16-bit digitizer and external 100 MHz 14-bit GAGE 8012A digitizer) which offer fast time resolution and a wide dynamic range as needed, and a personal computer to control the whole experiment.

* Corresponding author.

E-mail address: hongmei@iccas.ac.cn (H. Su).

The detector used in this experiment is a liquid nitrogen cooled InSb detector.

The reaction is initiated in a stainless steel flow reaction chamber. A pair of parallel multi-layer coated mirrors (reflectivity $R > 0.95$ at 248 nm) reflect the UV laser beam multiple times to increase the photolysis zone. CCl radicals are generated by 248 nm photodissociation ($100 \text{ mJ cm}^{-2} \text{ pulse}^{-1}$, 10 Hz repetition rate) of CCl_3Br . Samples of CCl_3Br ($\geq 99\%$) and O_2 ($\geq 99.5\%$) enter the flow chamber 1 cm above the photolysis beam via needle valves. The chamber is pumped by an 8 L s^{-1} mechanical pump and the stagnation pressure of the chamber is measured by a MKS capacitance monometer. The constant pressure of sample is maintained by adjusting the pumping speed and the needle valves. Transient infrared emission is collected by a pair of gold-coated White-Cell spherical mirrors and collimated by a CaF_2 lens to the step-scan Fourier spectrometer (Nicolet Nexus 870). The spectrometer and the collimating tube are both flushed with N_2 to prevent the environment CO_2 absorption. The spectral resolution is set at 16 cm^{-1} or at 0.5 cm^{-1} . The low resolution spectra are used to measure the rate constant of the reaction and the high resolution spectra are used to determine vibrational population of the product.

The detailed reaction mechanism is investigated theoretically with the GAUSSIAN 03 program package [11]. The geometric structures and vibrational frequencies for all stationary points are obtained using the DFT method at B3LYP/6-311G(d) level. The reaction paths are checked by performing intrinsic reaction coordinate (IRC) calculation [12], from which the quadratic steepest descent reaction paths are confirmed to connect the corresponding minima at the same level.

3. Results and discussion

3.1. Reaction products

The precursor molecule CCl_3Br was photolyzed by the KrF laser at 248 nm. In a reference experiment of pure photodissociation of CCl_3Br , no transient IR emission signal was found in the spectrum. Once the oxygen gas was mixed with CCl_3Br , strong IR emission was observed following the laser firing. As shown in Fig. 1, the IR emission intensity appears in a few microseconds and reaches its maximum intensity at $170 \mu\text{s}$. The emission intensity lasts for milliseconds. The only emission band spreading from 1950 cm^{-1} to 2200 cm^{-1} is assigned to a bunch of $\Delta v = -1$ vibrational transitions of CO. The high resolution spectrum consists of numerous rovibrational lines, further identifying the CO ($\nu \rightarrow \nu - 1$) assignment.

3.2. Identification of the $\text{CCl} + \text{O}_2$ reaction as a source of CO

In this experiment, CCl radicals were prepared by laser photolysis of CCl_3Br at 248 nm. Laser fluence dependence

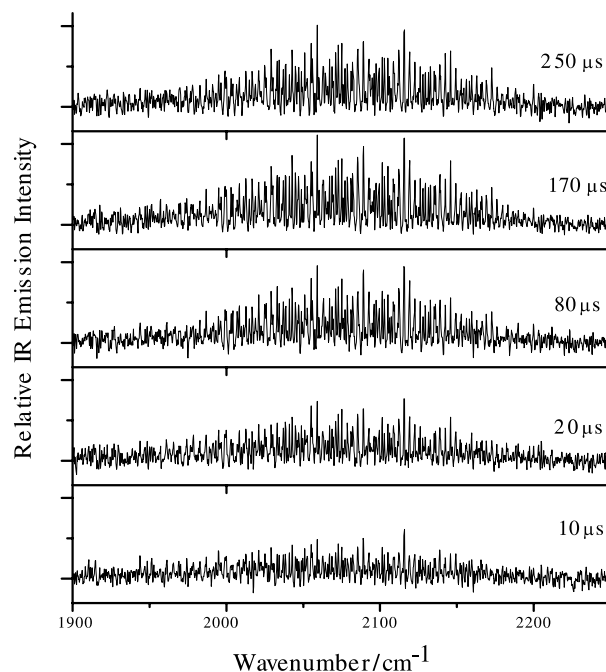
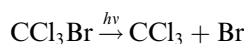


Fig. 1. Time-resolved FTIR emission spectra for the reaction $\text{CCl} + \text{O}_2$ with spectral resolution of 0.5 cm^{-1} at a series of reaction times after the KrF laser firing. The partial pressures of CCl_3Br and O_2 are 20 Pa and 80 Pa, respectively.

of CO yields have been measured in the intensities range of $3.7 \times 10^6 \text{ W cm}^{-2}$ and $8.9 \times 10^6 \text{ W cm}^{-2}$. The slope of the fluence dependence is 2.2 ± 0.2 indicating the product of CO is formed from a two-photon process. The primary photolytic process of CCl_3Br is [13]



Absorbing a second UV photon, the primary product CCl_3 can undergo a sequential photodissociation, yielding CCl or CCl_2 radicals:



or



Therefore, the two-photon photodissociation of CCl_3Br can generate a mixture of radicals containing CCl_3 , CCl_2 , CCl. A question arises as the following: which radical reacts with the abundant O_2 molecules to produce CO that we have observed? The room temperature rate constants for the three radical reactions are reported to be $2.91(\pm 0.144) \times 10^{-12} \text{ cm}^3 \text{ molecule}^{-1} \text{ s}^{-1}$ for $\text{CCl} + \text{O}_2$ [3], $3.01 \times 10^{-15} \text{ cm}^3 \text{ molecule}^{-1} \text{ s}^{-1}$ for $\text{CCl}_2 + \text{O}_2$ [3] and $3.3(\pm 0.2) \times 10^{-14} \text{ cm}^3 \text{ molecule}^{-1} \text{ s}^{-1}$ for $\text{CCl}_3 + \text{O}_2$ [14], respectively. The latter two reactions are two to three orders of magnitude slower than the $\text{CCl} + \text{O}_2$ reaction. The most reactive radicals are CCl and thus are the most likely to react with O_2 in the complex photochemical system.

3.3. Kinetics analysis

Fig. 2a plots the IR emission intensity of the peak area as a function of the reaction time within first 120 μs . Using pseudo-first order reaction rate equation to fit the rise of the IR emission from the product, the formation rates at various pressures are derived. It turns out that the formation rate is a linear function of O_2 pressure. From the slope of the line in Fig. 2b, the pseudo-first order rate constant is determined to be $2.6(\pm 0.4) \times 10^{-12} \text{ cm}^3 \text{ molecule}^{-1} \text{ s}^{-1}$. The rate constant agrees well with that measured previously which is at the range of $2.91(\pm 0.144) \times 10^{-12} \text{ cm}^3 \text{ molecule}^{-1} \text{ s}^{-1}$ [3] to $4.15(\pm 0.498) \times 10^{-12} \text{ cm}^3 \text{ molecule}^{-1} \text{ s}^{-1}$ [4]. The agreement further confirms that the $\text{CCl} + \text{O}_2$ reaction is the dominant radical reaction leading to the product CO.

In order to validate the above kinetics analysis, the effect of diffusion should be considered. Under our experimental conditions of 63 Pa of total pressure it is estimated that CO molecules diffuse only 4 mm away within 200 μs . Compared to the average observation zone of 3 cm, this distance is negligible. Therefore, the molecules are still in the observation zone on the time scale of hundreds of μs and the effect of diffusion can be neglected.

3.4. Vibrational energy disposal in CO

The reaction of $\text{CCl} + \text{O}_2$ is exothermic. The energy released deposits into different degrees of freedom of the products. The vibrational energy disposal of the product CO can be analyzed by fitting the IR spectra using a non-linear fitting program which has been described in detail elsewhere [15]. A simulated spectrum is shown in

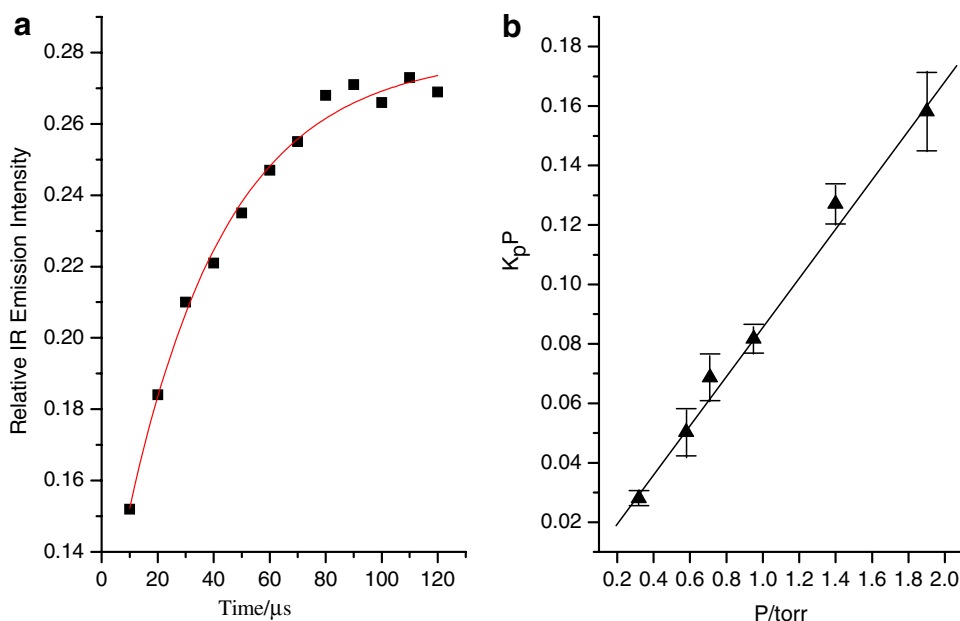


Fig. 2. (a) Plot of emission intensities as a function of reaction time. The partial pressures of CCl_3Br and O_2 are 20 Pa and 43 Pa, respectively. (b) The formation rates of CO as a function of O_2 pressure.

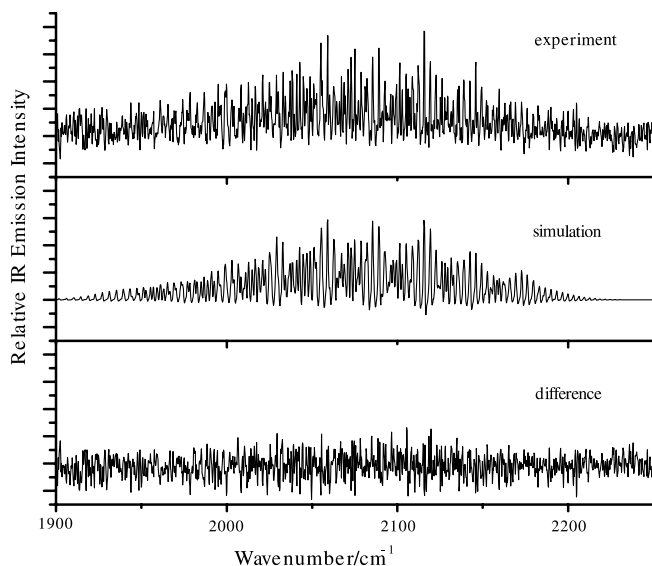
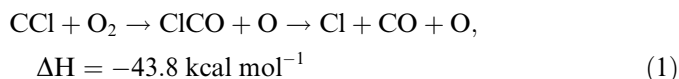


Fig. 3. Experimental and fitted CO IR emission spectra at the reaction time of 20 μs . The residual of the subtraction of the fitted spectra from experimental spectra is shown at the bottom.

Fig. 3. The simulation is calculated based on the rovibrational transitions of CO ($v \rightarrow v - 1$, $v = 1-7$). It can be seen that the simulated spectrum fits well with the experimental spectra. The best-fitted rotational temperature is nearly 300 K, the room temperature. This is reasonable because about 100 collisions take place within 20 μs at the total pressure of 100 Pa with the rotational excitation of the products being quenched completely. The vibrational excitation of CO sustains until milliseconds. This is due to the inefficient vibrational relaxation of CO. The colliding bath

Reaction time (μs)	10	20	40	60	170
E_v (kcal mol^{-1})	18.4	17.2	17.1	17.2	16.3

molecules O_2 and CCl_3Br in the system do not have any vibrational modes in resonance with the CO stretching (2140 cm^{-1}). By spectral fitting, the vibrational populations of CO are derived to be 1/0.92/0.91/0.59/0.38/0.21/0.13 for the vibrational level of $\nu = 1-7$ at $20\ \mu\text{s}$ reaction time. The vibrational population can be fitted nicely by a Boltzmann distribution with a vibrational temperature of $T_{\text{vib}} = 8700 \pm 1200\text{ K}$. The corresponding average vibrational energy is $17.2\text{ kcal mol}^{-1}$. Similarly, we fit the CO emission bands at different delay times. The average vibrational energy of CO (ν) at different reaction time is listed in Table 1. Obviously, the average vibrational energy of CO (ν) does not alter much with time. The nascent product CO should have an average vibrational energy of $17-18\text{ kcal mol}^{-1}$. There are two possible channels producing CO from the reaction of CCl radical with O_2 molecule:



Both channels are exothermic enough to produce vibrationally excited CO. It is not certain yet to judge which

channel mainly contribute to the formation of CO simply considering the energy disposal.

3.5. Reaction mechanism

In order to understand the reaction mechanism, DFT calculations are employed to elucidate the possible reaction paths. Energies and geometries of the reactants, intermediates and transition states on the doublet ground state are calculated and shown in Figs. 4 and 5. The calculation is performed at the B3LYP/6-311G(d) level. As shown in Fig. 4, the reaction starts with a barrierless addition reaction of O_2 to CCl, leading to a peroxide intermediate CICO (IM1). There are two possible paths linking the intermediate IM1 to the reaction product of CO, which has been observed in our experiment. The relatively feasible path is that the chain-like IM1 breaks its O–O bond and Cl–C bond sequentially via two transition states of TS1 and TS3, both corresponding to very low barriers. Therefore such sequential dissociation which corresponds to reaction channel (1) can take place easily. The large rate constant of the reaction is consistent with this mechanism. Starting from IM1, the second possible reaction path to produce CO involves much more complicated molecular rearrangements, including the formation of a $\text{C}\equiv\text{O}$ triple bond structure IM4 via transition states TS2 and TS4. IM4 dissociates to form ClO and CO by surmounting a fairly high barrier of $37.8\text{ kcal mol}^{-1}$ with the two terminal atoms Cl and O approaching to each other (TS5). This

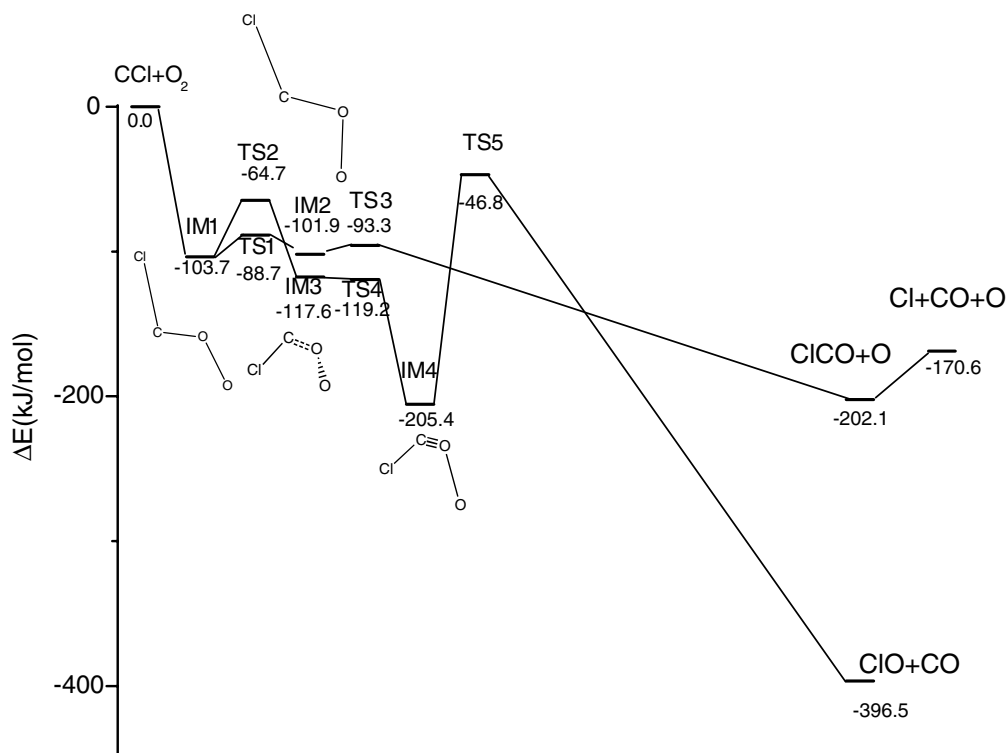


Fig. 4. Energy diagram for the $\text{CCl} + \text{O}_2$ reaction paths. The energies of the intermediates and transition states are calculated at the B3LYP/6-311G(d) level.

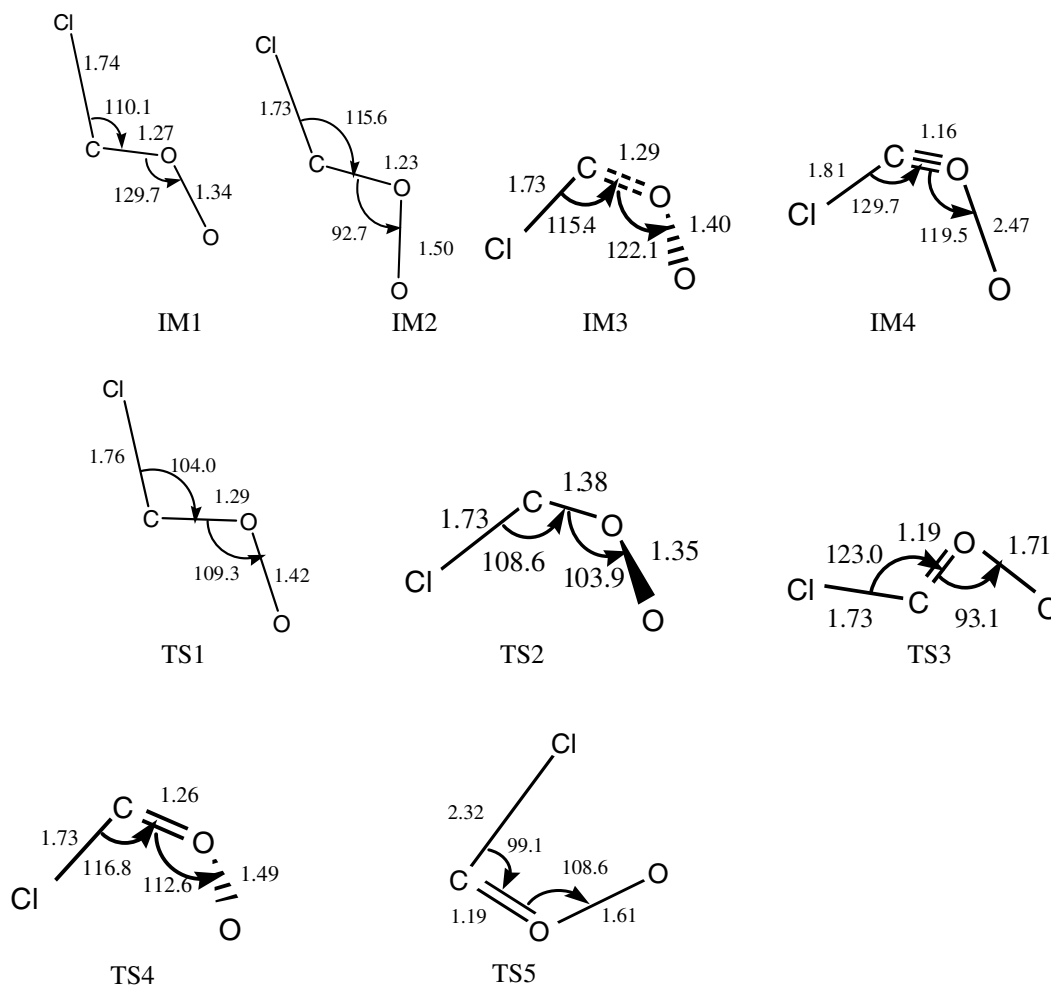


Fig. 5. Optimized structures of reactants, transition states, intermediates and products (bond length in angstrom and angle in degree) at the B3LYP/6-311G(d) level.

reaction path corresponds to reaction channel (2) which is much less favorable compared to the reaction channel (1) via sequential dissociation path. Therefore, the DFT calculation results show that the reaction channel (1) predominantly contributes to the production of CO. The reaction channel (1) releases $40.8 \text{ kcal mol}^{-1}$ of energy by calculation, which agrees well with the energy of $43.8 \text{ kcal mol}^{-1}$ calculated from experimental heat of formation. We observed that $17\text{--}18 \text{ kcal mol}^{-1}$ of energy is partitioned into the vibration of CO, indicating that a fairly high fraction of internal energy. This is consistent with the low exit barrier of this reaction channel in the reaction path.

4. Conclusions

The elementary reaction products, channels, rate constants and vibrational energy disposal of CCl with O₂ have been investigated by TR-FTIR emission spectroscopy. In combination with DFT calculations, the major reaction channel is elucidated to be a sequential dissociation of $\text{CCl} + \text{O}_2 \rightarrow \text{ClCO} + \text{O} \rightarrow \text{Cl} + \text{CO} + \text{O}$ via an addition–

elimination mechanism by first forming a ClCOO peroxy intermediate.

Acknowledgement

This work is financially supported by the National Natural Science Foundation of China (Grant Nos. 20473100 and 20673126) and the Chinese Academy of Sciences.

References

- [1] WMO Global Ozone Research and Monitoring Project, Report No. 20, 1989.
- [2] S.M. Senkan, Detoxification of Hazardous Waste, Chapter 3, 1982.
- [3] J.J. Tiee, F.B. Wampler, W.W. Rice Jr., Chem. Phys. Lett. 73 (1980) 519.
- [4] W.J.R. Tyerman, J. Chem. Soc. A (1969) 2483.
- [5] Z.X. Wang, M.B. Huang, J. Mol. Struct: Theochem. 491 (1999) 223.
- [6] P. Jin, B.C. Chang, R. Fei, T.J. Sears, J. Mol. Spectrosc. 182 (1997) 189.
- [7] R.D. Johnson, J. Chem. Phys. 96 (1992) 4073.
- [8] C.J. Reid, Chem. Phys. 210 (1996) 501.
- [9] F.C. James, H.K.J. Choi, O.P. Strausz, T.N. Bell, Chem. Phys. Lett. 68 (1979) 131.

- [10] P.W. Seakins, *The Chemical Dynamics and Kinetics of Small Radicals*, in: K. Liu, A. Wagner (Eds.), World Scientific, Singapore, 1995, p. 250.
- [11] M.J. Frisch et al., *GAUSSIAN 03*, Revision B.01, Gaussian, Inc., Pittsburgh PA, 2003.
- [12] C. Gonzalez, H.B. Schlegel, *J. Phys. Chem.* 94 (1990) 5523.
- [13] Y.R. Lee, W.B. Tzeng, Y.J. Yang, Y.Y. Lin, S.M. Lin, *Chem. Phys. Lett.* 222 (1994) 141.
- [14] T. Imamura, H. Chono, K. Shibuya, N. Washida, *Int. J. Chem. Kinet.* 35 (2003) 310.
- [15] H. Su, J. Yang, Y. Ding, W. Feng, F. Kong, *Chem. Phys. Lett.* 326 (2000) 73.